Journal of the European Ceramic Society **19** (1999) 1789–1793

PII: S0955-2219(98)00280-5
0955-2219/99/$ - see front matter

SiC–AlN Particulate Composite

Yu-bai Pan,[a]* Jian-hui Qiu,[a] Makoto Kawagoe,[a] Mikio Morita,[a] Shou-hong Tan[b] and Dong-liang Jiang[b]

[a]Faculty of Engineering, Toyama Prefectural University, 5180 Kurokawa, Kosugi, Toyama 939-0398, Japan
[b]Shanghai Institute of Ceramics, Chinese Academy, 1295 Road, Shanghai 20050, People's Republic of China

(Received 14 July 1998; accepted 13 November 1998)

Abstract

A SiC–AlN composite was fabricated by mechanical mixing of SiC and AlN powders, hot pressed under 40 MPa at 1950°C in Ar atmosphere. The object of this attempt was to achieve full density and a little solid solution formation. Fine microstructure and crack deflection behaviour are to improve the mechanical properties of the SiC–AlN composite. The bending strength and fracture toughness were achieved 800 MPa and 7·6 MPa $m^{1/2}$ at room temperature, respectively. The fracture toughness of the SiC–AlN composite shows minimal change between room temperature and 1400°C. Post-HIP improves the surface densification of the SiC–AlN composite resulting in an increase of the strength and the ability to resist oxidization. The bending strength of SiC–AlN composite increases from 800 to 1170 MPa after HIP treatment for 1 h under 187 MPa at 1700°C in N_2 atmosphere. © *1999 Elsevier Science Limited. All rights reserved*

Keywords: AlN, composites, SiC, mechanical properties, corrosion.

1 Introduction

Silicon carbide is an attractive candidate material for many structural applications. However, strength, reliability and fracture toughness of SiC still represents limitations for some applications. This disadvantage prevents the practical use of silicon carbide as a high performance structural material. To overcome these disadvantages, SiC composites were developed since some years ago.[1] The important step in the design of a SiC matrix composite is to define the selection of the second phase particle and the formation feasibility of SiC–AlN composites. Since Cutler and Miller found that 2H polymorph of SiC and AlN can form solid solution,[2] much of the research has focused on a SiC–AlN binary system.[3,4] Although the strengths and toughness of SiC–AlN solid solution,[5,7] when compared with SiC ceramics, were quite low with little improvement, but it is interesting that AlN was found to inhibit grain growth of SiC.[6] Based on a tentative SiC–AlN phase diagram[4] and publication literatures, SiC–AlN particulate composites were fabricated by mechanical mixing of the SiC and AlN powders, and then hot-pressed at 1950°C under 40 MPa for 0·5 h. This was done in an attempt to achieve full density and to form partial solid solution, as well as retain steep compositional gradients. Its microstructure would be used to reinforce and toughen the SiC–AlN particulate composite.

2 Experimental Procedure

AlN with an average particle size of 3 μm was used as the reinforcing and toughening particles. Powder of monolithic α-SiC of 0·6 μm was mixed with AlN and Y_2O_3, by ball milling for 10 h. The composition: SiC:AlN:Y_2O_3 (weight ratio) was 85:14.5:0·5, in which the Y_2O_3 was added as a sintering aid. The SiC/AlN mixtures were then hot-pressed to dense materials at 1950°C under 40 MPa in Ar atmosphere. Some of these sintered samples would be treated by hot isostatic pressing (HIP) for 1 h under 187 MPa at 1700°C in N_2 atmosphere.

The strengths at both room temperature and high temperature were measured by three-point bending test with a specimen size of $3\times4\times36$ mm^3. The tests were conducted on an Instron material testing machine, the deformation rate were 0·5 mm/min. The span is 30 mm in the bending strength measurement. The fracture toughness of the materials was evaluated by single edge notch beam (SENB) with a specimen size of $2{\cdot}5\times5\times24$ mm^3,

*To whom correspondence should be addressed.

the deformation rate of 0·05 mm/min. The depth and width of the specimen notch is 2·5 and less than 0·2 mm, respectively. The span is 20 mm in the measurement of the fracture toughness. Both the measurement of the bending strength and fracture toughness, eight pieces of specimens were measured at room temperature and three pieces of specimens were done at each point of high temperature.

The microstructures, cracks, fracture surfaces and boundary interfaces of SiC–AlN specimens were observed by scanning electron microscope (SEM) equipped with energy dispersive X-ray spectroscopy (EDXS) and transmission electron microscopy (TEM) with an energy-dispersive X-ray spectrometer (EDS) for elemental analysis.

3 Results and Discussion

During the sintering process, SiC and AlN will be vapourized at high temperature, and produce diffusion in the compact surface. The rate of transport from a surface is taken to be proportional to the equilibrium vapour pressure over the surface. The solid vapourization pressures of AlN and SiC achieve 14 and $1{\cdot}23\times10^{-3}$ mm Hg at 1900°C.[8] Thus, the material transport rate from AlN to SiC is faster than the opposing process at high temperature.

Theoretical considerations indicate that the density of packing of atoms along grain boundaries is smaller than in the bulk of crystal. This suggests that the activation energy of diffusion along grain boundaries should be lower than that of lattice diffusion and consequently the rate of intergranular diffusion should be faster. The rate of diffusion is determined by self-diffusion of the grains.

The Arhenius relationship, generally applicable to all branches of chemical kinetics, is also a valid description of the temperature dependence of the diffusion coefficient.

$$D = D_0 e^{-Q/RT} \tag{1}$$

where D_0 is a frequency factor which a temperature independent constant, R is the gas constant, T is temperature, and Q the activation energy.

One simple experiential equation[9] but successful examples of such rules are given below, where T_m is the melting temperature.

$$Q_{\mathrm{D}} = 33{\cdot}7T_m \tag{2}$$

The self-diffusion coefficient:

$$D = 3{\cdot}4 \times 10^{-5} T_m a_0^2 \exp(-17T_m/T) \tag{3}$$

Where

D:	diffusion coefficient ($cm^2\,s^{-1}$)
D_0:	frequency factor ($cm^2\,s^{-1}$)
a_0:	lattice constant expressed in nm ($0{\cdot}1\times10^{-9}$)
T:	temperature in the Kelvin scale
T_m:	melting point in the Kelvin scale.

Because there are no melting temperatures for SiC and AlN, the decomposition temperatures, which SiC is 2830°C and AlN is 2400°C,[10] are assumed for T_m. Therefore, the self-diffusion of SiC and AlN at 1950°C can be estimated at $4{\cdot}95\times10^{-13}$ and $1{\cdot}17\times10^{-11}$ $cm^2\,sec^{-1}$, respectively. The diffusion ability of AlN is about 24 times greater than that of SiC. As there is much AlN existing in boundaries, it results in a decrease in sintering temperature as compared with monolithic α-SiC ceramics. SiC–AlN can be sintered at 1950°C under 40 MPa for 0·5 h in Air atmosphere.

The system of SiC-AlN passes through three steps to form the solid solution at the end. Initially, the AlN particle is vapourized from its own surface Next, AlN vapour is deposited onto the surface of the SiC grains and the AlN particle due to vapourization accompanied with reduction in the size of itself. Finally, the formation of partial SiC–AlN solid solution occurs at the boundary of the SiC grains. As a result of the AlN deposition and solid solution formation in the boundary of the SiC grains, a barrier layer is formed on the surface of SiC grains. This result leads to the formation of fine grains.[11] Figure 1 shows the fracture surface of SiC–AlN composite.

Two aspects of the toughening model are explained in this study: (1) the thermal expansion of SiC and AlN are $4{\cdot}5\times10^{-6}$ (room temperature to 2200°C) and $6{\cdot}09\times10^{-6}$/K (room temperature to 2000°C), respectively. There is compressive stress around SiC grains. It therefore favours the

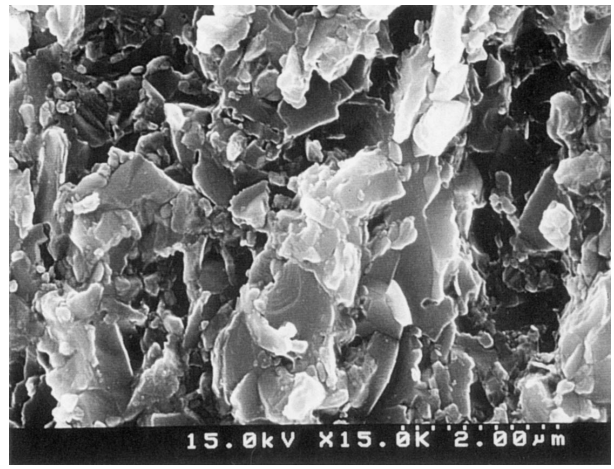

Fig. 1. The fracture surface of SiC–AlN composite.

mechanisms of toughening by crack deflection ($\alpha_p > \alpha_m$). (2) for a weak interface of SiC–AlN solid solution, a crack in the SiC matrix can lead to debonding at the interface, followed by crack deflection. Additional energy-absorbing phenomena lead to an enhanced fracture toughness. Figure 2 is expressed as the crack deflection behavior of SiC–AlN composite.

Figure 3 shows the mechanical properties of the SiC–AlN composite between room temperature and 1400°C. The microstructure of the composite weakens at high temperature as the microhardness decreases linearly from room temperature to 1200°C,[12] as shown in Fig. 4.

On the other hand, because the mechanical properties of SiC–AlN solid solution are lower, the SiC–AlN composite maintains its fracture toughness, probably due to a weakening of the boundaries. For these reasons, not only does ΔT decrease resulting in the stress around the grain-boundaries also decreasing, but the fracture toughness of SiC–AlN composites has minimal change between room temperature and 1400°C, as shown in Fig. 3.

This is unlike the case of transformation toughening of zirconia. The toughness of ZrO_2 is observed to fall continuously with increasing temperature due to a loss of the transformation.

Pores, inclusions, and other inherent internal defect as well as roughness, surface flaws, or other external defects influence the strength of ceramic materials. The presence of a flaw in a ceramic material results in stress concentration. Equation

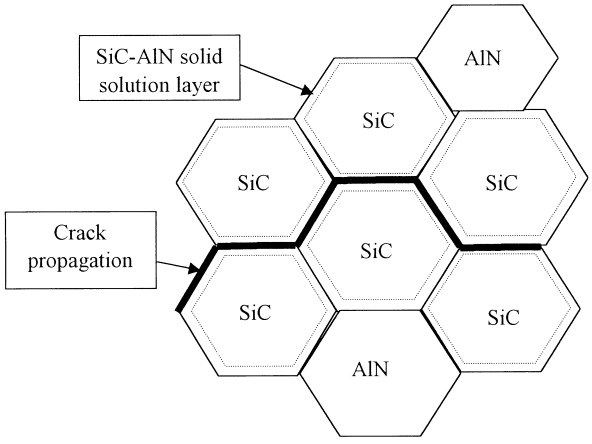

Fig. 2. The schematic representation for crack deflection.

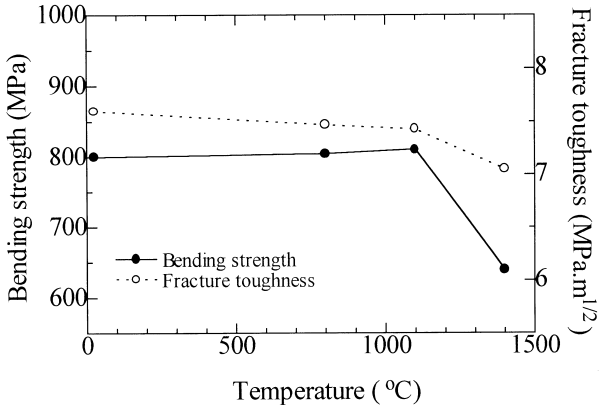

Fig. 3. The mechanical properties of SiC–AlN composite from room to high temperature.

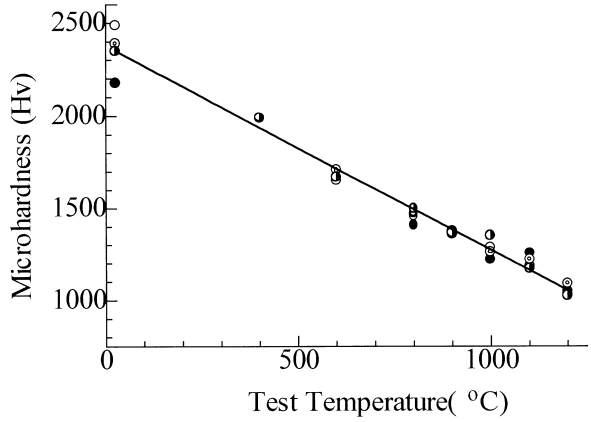

Fig. 4. The microhardness of SiC–AlN composite from room to high temperature.

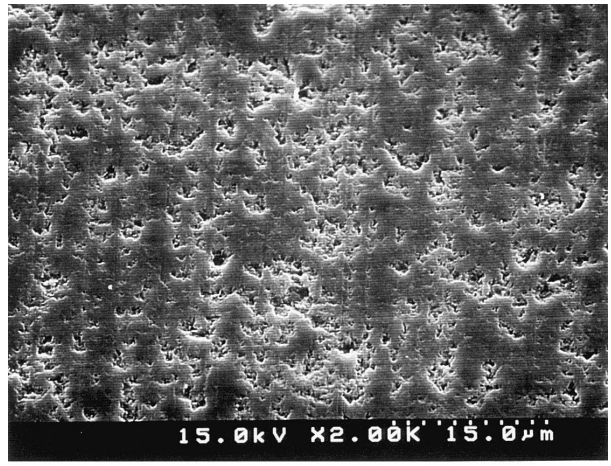

(a) The surface of HP sample A

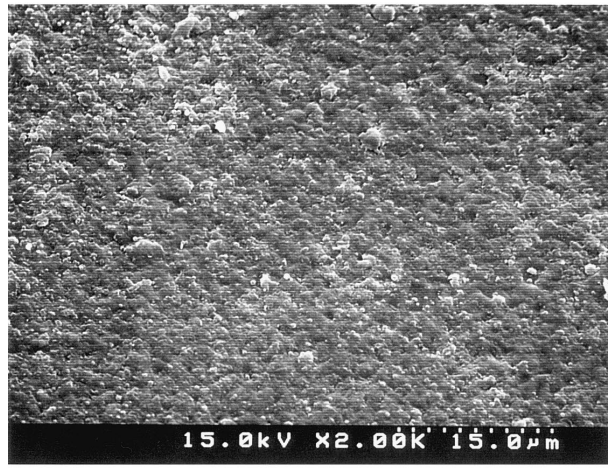

(b) The surface of HIP sample B

Fig. 5. The SEM photograph of SiC–AlN composite. (a) The surface of HP sample A; (b) the surface of HIP sample B.

(4) presents a more general relationship between strength and flaw:

$$\sigma_f = \frac{Z}{Y}\left(\frac{2E\gamma}{c}\right)^{1/2} \quad (4)$$

where Y is a dimensionless term that depends on the flaw depth and test geometry, Z is another dimensionless term that depends on the flaw configuration, c is the depth of surface flaw, and E and γ are defined as the elastic modulus and the fracture energy, respectively.

Post-HIP with the external load was superimposed on the intrinsic sintering pressure. Mass transport results in flaw and pore elimination in the final densification stage. Pores and flaws can be also eliminated from the surface when the microstructure was presintered to close porosity.

As a result of observation, it could clearly be seen that the surface of HP Sample A was different in the surface of post-HIP Sample B. The SEM images of these surfaces are shown in Fig. 5.

Comparing A with B, the mechanical properties increase as a result of post-HIP, especially in the bending strength, as shown in Table 1.

SiC–AlN composites by HP and HIP were oxidized at temperature of 1100, 1250 and 1370°C for 30 h in air. The size of the specimens was $5\times5\times10\,mm^3$. Figure 6 shows the weight gain as result of oxidization versus time at various temperatures for the SiC–AlN composite. As the surface is more dense after HIP treats. The oxidization resistance ability of the SiC–AlN is significantly improved. The effect of oxidization resistance by post-HIP is clearly seen at 1250 and 1370°C.

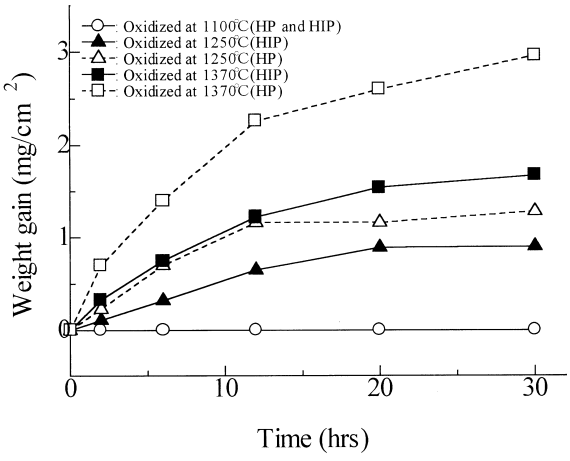

Fig. 6. The weight gain as result of oxidization of HP and HIP SiC–AlN composites at various times and temperatures.

Table 1. The properties of HP and post-HIP

Type	*Density* ($g\ cm^{-3}$)[a]	*Bending strength (MPa)*
HP (A)	3·1983	800 ± 73
Post-HIP (B)	3·2005	1170 ± 45

[a]SD-222L (Mirage Trading Co., Ltd., made in Japan)

4 Conclusion

The fracture toughness results indicate that there is significant toughening due to the addition of AlN particles to a SiC matrix. The solid solution layer of SiC–AlN on the grain surfaces restricts the excessive growth of SiC crystal grains and forms a fine microstructure. Two aspects effective toughening are that there is compressive stress around the SiC grains due to a thermal expansion mismatch and a weak interface of SiC–AlN solid solution. The fine microstructure and crack deflection behavior help improve the mechanical properties of the SiC–AlN composite. The bending strength is 800 MPa at room temperature and 640 MPa at 1400°C. The fracture toughness is 7·6 MPa $m^{1/2}$ at room temperature. The fracture toughness of the SiC–AlN composite insignificantly changes between room temperature and 1400°C.

The SiC–AlN composite can be further densified on the surface by post-HIP. Through post-HIP, pores and flaws on the sample surface can be eliminated thus achieving better densification on the surface. Post-HIP improved the resistance to oxidization of the SiC–AlN composite. Post-HIP contributed to the increase in the bending strength of SiC–AlN composite at room temperature. It increased from 800 to 1170 MPa.

Acknowledgement

The authors would like to thank Mrs Megumi Nomiya for her assistance in the SEM operation.

References

1. Jiang, D. L., Silicon carbide based composites. *China J. Inorganic Materials*, 1995, **10**, 151–163.
2. Cutler, I. B., Miller, P. D., Rafaniello, W., Park, H. K., Thompson, D. P. and Jack, K. H., New material in the Si–C–Al–O–N and related system. *Nature*, 1978, **275**, 434–435.
3. Rafaniello, W., Plichta, M. R. and Virkar, A. V., Investigation of phase stability in the system SiC–AlN. *J. Am. Ceram. Soc.*, 1983, **64**, 272–276.
4. Zangil, A. and Ruh, R., Phase relationships in the silicon carbide–aluminum nitride system. *J. Am. Ceram. Soc.*, 1988, **71**, 884–890.
5. Rafaniello, W., Cho, K. and Virkar, A. V., Fabrication and characterization of SiC–AlN alloys. *J. Mater. Sci.*, 1981, **16**, 3479–3488.
6. Ruh, R. and Avigdor, Z., Composition and properties of hot-pressed SiC–AlN solid solution. *J. Am. Ceram. Soc.*, 1982, **65**, 260–265.

7. Lee, R.-R. and Wei, W.-C., Fabrication, microstructure, and properties of SiC–AlN ceramic alloys. *Ceram. Erng. Sci. Proc.*, 1990, **11**, 1094–1121.
8. Camcohob, P. B., *Handbook of High-melting Point Compound*. China Industry, 1965, pp. 110–115.
9. Mrowec, S., *Defects and Diffusion in Solid*. Elsevier/North Holland, Amsterdam, 1974, pp. 174–286.
10. Suita, S. and Kawarmoto, K. *Material Technology–Ceramic Materials*. Japan Tokyo University, Tokyo, 1986.
11. Pan, Y. B, Qiu, J. H., Morita, M., Tan, S. H. and Jiang, D. L., The mechanical properties and microstructure of SiC–AlN particulate composite. *J. Mater. Sci.*, 1998, **33**, 1233–1237.
12. Pan, Y. B., Qiu, J. H. and Morita, M., Oxidization and microhardness of SiC–AlN composite at high temperature. *Mater. Res. Bull.*, 1998, **33**, 133–139.